RSC Advances

PAPER

View Article Online
View Journal | View Issue

Cite this: *RSC Adv.*, 2022, **12**, 31699

Renewable green reactive diluent for bisphenol a epoxy resin system: curing kinetics and properties

Jingyu Li, [ab] Haichao Zhao [*c] and Guoxin Sui [*ab]

Hydrosilylation epoxidized eugenol (HSI-EP-EU) is successfully synthesized and used as a reactive diluent for epoxy/anhydride (marked as P) and epoxy/imidazole (marked as I) curing systems. The reactive bio-based diluent HSI-EP-EU has an excellent dilution effect on petroleum-based epoxy resin (E44). The curing kinetics of P + HSI-EP-EU and I + HSI-EP-EU are studied by a non-isothermal DSC method. The kinetics parameters are calculated by using the Kissinger model, Crnae model, Ozawa model and β-T (temperature-heating speed) extrapolation, respectively, to determine theoretically reasonable curing conditions. In addition, the effects of HSI-EP-EU on the antibacterial properties, thermo-mechanical properties and thermal stability of P + HSI-EP-EU and I + HSI-EP-EU systems are also studied. It is found that HSI-EP-EU possessed obvious antibacterial properties and could effectively improve the mechanical properties for the I + HSI-EP-EU.

Received 17th August 2022
Accepted 24th October 2022

DOI: 10.1039/d2ra05160e

rsc.li/rsc-advances

Introduction

Epoxy resin and epoxy resin matrix composites[1] are widely used in aerospace,[2] building materials,[3] sports equipment,[4] biomaterials,[5] adhesives,[6] coatings[7] and other defense and civilian products,[8] due to their excellent adhesion, mechanical properties and thermal stability.[9] Compared with other thermosetting materials, epoxy resin has relatively good processing properties, but in fact the viscosity of epoxy resin is still high at room temperature, and researchers are also working to further improve the processing properties of epoxy resin.[10] Organic solvents are often used to reduce the viscosity of petroleum-based bisphenol A epoxy resin curing systems. The epoxy resin diluents are dibutyl phthalate, dioctyl phthalate, styrene, diallyl phthalate, toluene, xylene and other volatile liquids.[11,12] However, most organic solvents are poisonous chemicals. What's more, they also cause serious environmental pollution and result in a substantial loss of petroleum resources. More and more environmental concerns and strict regulations give a push to the reduction of volatile organic compounds (VOC).[13]

Sustainable development[14] focuses on the long-term tolerance of the Earth to the development of human society, with a view to reduce the negative impact of human activities on the natural environmental sustainability. Based on the concept of sustainable development, as one of the most popular research directions, green chemistry[15] is becoming an industrial and academic chemistry. For epoxy diluents, most researchers currently focus on the dilution effect of the diluent and ignore the reactivity of the diluent itself. Such diluents[16] usually include butyl glycidyl ether, benzyl glycidyl ether, allyl glycidyl ether, dodecyl and tetradecyl glycidyl ethers, 1,4-butanediol diglycidyl ether, *etc.* The use of renewable resources as raw materials to prepare reactive bio-based epoxy diluents by conventional synthetic processes is one of the continuous research directions in the field of thermosetting resin modification.[11] The reactive bio-based epoxy diluents can participate in the curing reaction. However, the existing resin diluent is difficult to have both high biological content and excellent performance. This topic will produce a reactive bio-based diluent that combines high biomass and high comprehensive performance to solve the above problem.

Functionalized vegetable oils have been reported as renewable resourced toughening diluents for epoxy to overcome its inherent brittleness. For instance, Sahoo[17] has developed the renewable resourced toughened epoxy blend using epoxidized linseed oil (ELO) and bio-based crosslinker. ELO can effectively reduce the viscosity of epoxy resin and increase processing performance. The bio-epoxy blend with 20 to 30 phr of ELO shows moderate stiffness with much higher elongation at break. Plant polysaccharides can also be used to modify epoxy resins. Hu[18] holds the opinion that furans derived from cellulose and hemicellulose are promising candidates for phenyl substitution and have been shown to be viable building blocks for renewable high-performance epoxy resins. Ding[19] has reported a reactive epoxy diluent of furfuryl glycidyl ether (FGE). When the content of FGE is 10 wt%, the tensile modulus and

[a]*Institute of Metal Research, Chinese Academy of Sciences, Shenyang 110016, China. E-mail: gxsui@imr.ac.cn*

[b]*School of Materials Science and Engineering, University of Science and Technology of China, Hefei 230000, China*

[c]*Key Laboratory of Marine Materials and Related Technologies, Zhejiang Key Laboratory of Marine Materials and Protective Technologies, Ningbo Institute of Materials Technology and Engineering, Chinese Academy of Sciences, Ningbo 315201, P. R. China. E-mail: zhaohaichao@nimte.ac.cn*

flexural modulus of epoxy system is increased 16.2% and 16.4%, respectively. Huang[20] has made a thorough inquiry of the feasibility for bio-based maleopimarate as an alternative to petrochemical-based trimellitic anhydride.

Eugenol, a monolignol commonly obtained from cloves, is widely used in perfumes, cosmetics, biomedical, taste and food additives.[21,22] Chen[11] has synthesized monoglycidyl silyl etherated eugenol (GSE) reactive epoxy diluent and finds that the GSE not only effectively improved the processing properties of the anhydride-cured epoxy resin system, but also improved the thermal stability and toughness of the cured product. Li[23] has reported a new silicone-bridged difunctional epoxy monomers exhibiting much lower viscosity (<2.5 Pa s) than commercial DGEBA epoxy (10.7 Pa s) suitable for composites and prepregs. The cured product exhibits a dielectric permittivity as 2.8 and the intrinsic flame retardancy is far outperforming DGEBA. Qin[24] has prepared an eugenol-based epoxy, and shows that they have similar reactivity, dynamic mechanical properties and thermal stability between eugenol-based epoxy and the bisphenol A type epoxy. François[25] uses the biobased diepoxy synthons derived from isoeugenol, eugenol or resorcinol as epoxy monomers in replacement of the diglycidyl ether of bisphenol A (DGEBA). These cured materials exhibit interesting thermal and mechanical properties comparable with conventional petro-sourced DGEBA-based epoxy resins cured in similar conditions. At present, the research on eugenol-based epoxy resin diluent mainly focuses on its reactivity and the diluting effect on epoxy resin, but ignores the positive effect of eugenol on the cured material in the field of biological antibacterial.

Infectious disease prevention and treatment is a permanent global challenge. Some clinical diseases are associated with bacterial microbial infections.[26] Developing epoxy resin with excellent processability, adding non-reactive diluent may deteriorate the original properties of the material.[27] We believe that the preparation of eugenol-based epoxy resin diluent using the antibacterial effect of eugenol can impart antibacterial function to epoxy resin materials. In this work, a synthesized reactive diluent is investigated the effect on processability of conventional petroleum-based bisphenol A epoxy resins. The addition of reactive diluent not only greatly improves the processing properties of epoxy prepolymers, but also participates in the curing reaction. We also study the optimum process parameters when diluent is used in epoxy/anhydride and epoxy/imidazole curing system, and explore the mechanical properties, thermal mechanical properties and antibacterial properties of cured products prepared with the optimum process parameters.

Materials and methods

Materials

Eugenol (99%), triethylsilane (98%), benzyltriethylammonium chloride (TEBAC, 98%), (±)-epichlorohydrin (AR), 2,4,6-tris(dimethylaminomethyl)phenol (DMP-30, 95%), 1-methylimidazole (NMI, 99%), *cis*-1,2-cyclohexanedicarboxylic anhydride (HHPA, 99%), aluminum oxide, Karstedt Catalyst Solution (2%) and glutaraldehyde solution (2.5 vol%) were purchased from Shanghai Aladdin Industrial Co., Ltd. Epoxy resin (E-44) was provided by Jiangsu Heli coating Co., Ltd. Calcein-AM/PI Double Stain Kit 40747ES76 was obtained from Shanghai Yeasen Biotechnology Co., Ltd, (Shanghai, china). Centrifuge tubes, sterile culture dishes, pipettes and pipette tips, sterile well plates, semipermeable membrane, *etc.* were purchased from Ningbo Zhenhai Hangjing Biotechnology Co., Ltd, (Ningbo, Zhejiang, China). Nutrient agar, LB broth, 2216E liquid medium and 2216E agar were purchased from Qingdao Hope Bio-Technology Co., Ltd, (Qingdao, Shandong, China). *Escherichia coli* (ATCC 25922) and *Bacillus subtilis* ATCC6633 were provided by Shanghai Luwei Technology Co., Ltd, (Shanghai, china). All other chemicals and reagents were analytical grade and used as received without further purification.

Synthesis of epoxidized eugenol (EP-EU)

Scheme 1 has shown the synthetic route of EP-EU. We firstly conducted the reaction of eugenol with epichlorohydrin at a mol ratio of 1 : 6 (eugenol *versus* epichlorohydrin) to a 250 mL round-bottom flask equipped with a magnetic stirrer and a condenser. Eugenol (16.42 g, 0.1 mol), epichlorohydrin (55.51 g, 0.6 mol) and benzyltriethylammonium chloride (2.27 g, 0.01 mol) were added and reacted in order to fully connect the epichlorohydrin to the phenyl hydroxyl group of eugenol under nitrogen flow at 110 °C reflux for 2 h. Then, the temperature was reduced to 70 °C and sodium hydroxide aqueous solution (4.10 g, 0.103 mol, 20 wt%) was dropped into the mixture in the period of 10 h. The final mixture was separated into two layers, the upper organic layer and the lower water phase layer. The above two-layered liquid in a separatory funnel was placed and poured out the upper organic layer. The organic layer was washed with saturated saline for 3 times, then dried with Na_2SO_4 for 24 h. The excessive epichlorohydrin was removed by distillation under reduced pressure to obtain crude product 1. The crude product 1 was mixed with an appropriate amount of methanol and placed in a refrigerator at −5 °C for 24 h. The filtered precipitate was obtained a yellowish liquid EP-EU (yield: 79%) under reduced pressure.

Eugenol ^{1}H NMR (400 MHz, $CDCl_3$) $\delta = 6.86$ (benzene ring, 1H), 6.84 (benzene ring, 1H), 6.69 (benzene ring, 1H), 5.95 (=CH–, 1H), 5.54 (–OH, 1H), 5.07 (=CH_2, 1H), 5.04 (=CH_2, 1H), 3.87(–CH_3, 3H), 3.31 (–CH_2–, 2H) ppm; (EP-EU) ^{1}H NMR (400 MHz, $CDCl_3$) $\delta = 6.97$ (benzene ring, 1H), 6.84 (benzene ring, 1H), 6.71 (benzene ring, 1H), $\delta = 5.59$ (=CH–, 1H), 5.01 (=CH_2, 2H), 4.20 (–CH_2, 1H), 4.01 (–CH_2–, 1H), 3.85(–CH_3, 3H), 3.37 (–CH_2–, 2H), 3.31(–CH–, 1H), 2.87 (–CH_2–, 1H), 2.72 (–CH_2–, 1H) ppm.

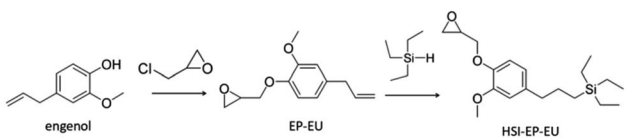

Scheme 1 Synthesis route of Hydrosilylation epoxidized eugenol (HSI-EP-EU).

Synthesis of hydrosilylation epoxidized eugenol (HSI-EP-EU)

HSI-EP-EU was prepared from EP-EU as following procedure. The reaction of EP-EU (22.02 g, 0.1 mol) with triethylsilane (17.42 g, 0.15 mol) was conducted at a mol ratio of 1 : 1.5 (EP-EU *versus* triethylsilane) to a 50 mL round-bottom flask (karstedt catalyst solution catalyst: 10 ppm) equipped with a magnetic stirrer and a condenser. Then, the temperature was maintained at 100 °C, and triethylsilane was dropped into the mixture in 2 h. The reaction was taken for another 5 h to end the reaction and cooled down to the room temperature. Both xylene from the karstedt catalyst solution and the excess triethylsilane was then removed by distillation under reduced pressure. The resulting oil was purified by flash column chromatography (ethyl acetate/hexane, gradient 0–100% hexane) and dried under vacuum overnight to afford the title product as a clear, red-brown liquid (yield 87%). Epoxy value was 0.28. ^{1}H NMR (400 MHz, $CDCl_3$): δ = 6.88 (benzene ring, 1H), 6.83 (benzene ring, 1H) 6.70 (benzene ring, 1H), 4.19 (–CH_2–, 1H), 4.01 (–CH_2–, 1H) 3.85 (–CH_3, 3H), 3.37 (–CH–, 1H), 2.88 (–CH_2–, 1H), 2.71 (–CH_2–, 1H), 2.55 (–CH_2–, 1H), 1.85 (–CH_2–, 2H), 0.90 (–CH_3, 9H), 0.50 (–CH_2–, 8H) ppm.

Preparation of cured P + HSI-EP-EU polymer

Scheme 2 has shown the curing mechanism of the P + HSI-EP-EU. The acid anhydride curing agent HHPA (7.6 g) and DMP-30 curing accelerators (0.19 g) were dissolved in HSI-EP-EU (1.76 g), and the mixture was added to EP-44 (10 g) and heated to 60 °C for 10 min to be homogeneously mixed. The compound was degassed under vacuum and then poured into a Teflon mold and cured at the given temperature.

Preparation of cured I + HSI-EP-EU polymer

Scheme 3 has shown the curing mechanism of the I + HSI-EP-EU system. The curing agent NMI (0.8 g) was suspended in HSI-EP-EU (1.76 g), and the mixture was added to EP-44 (10 g) and stirred for 20 min at 60 °C. The compound was degassed under vacuum and then poured into a Teflon mold and cured at the given temperature.

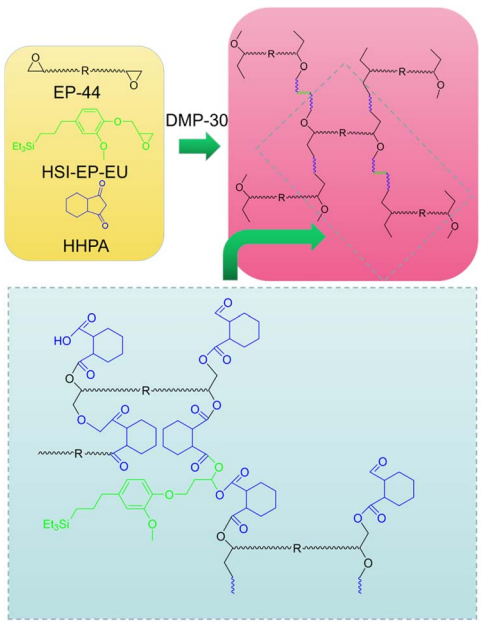

Scheme 2 The structure of cured P + HSI-EP-EU polymer network.

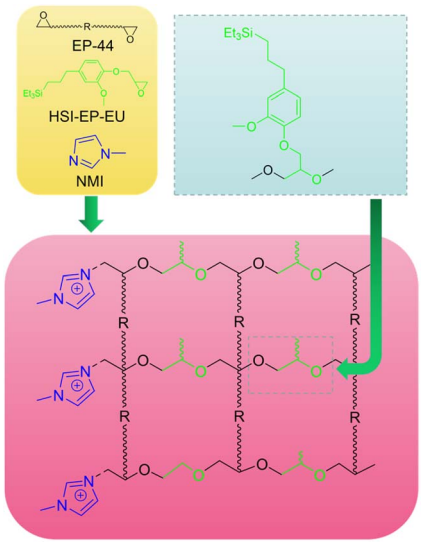

Scheme 3 The structure of cured I + HSI-EP-EU polymer network.

Antibacterial property test of HSI-EP-EU, cured P + HSI-EP-EU polymer and cured I + HSI-EP-EU polymer

Enterobacteria *Escherichia coli* (ATCC 25922) and marine bacteria *Bacillus subtilis* (ATCC6633) were chosen for the HSI-EP-EU antibacterial activity assessment by the zone of inhibition and shaking flask coated plate method.

The implementation of the zone of inhibition method was carried out according to the following steps. The 50 μL HSI-EP-EU was dropped onto the surface of an agar plate contained about 10^6 CFU mL^{-1} of bacteria, then incubated at 37 °C for 24 h. For the *Bacillus subtilis*, 2216E agar was used to replace nutrient agar.

The implementation of the shaking flask coated plate method was carried out according to the following steps. To determine the anti-*bacillus subtilis* activity of the HSI-EP-EU, a certain volume of *Bacillus subtilis* suspensions were added into the sterilized natural seawater to make sure the bacteria concentration was about 10^4 CFU mL^{-1} in a conical flask. Then, the 100 μL HSI-EP-EU was added into the 40 mL above bacteria suspensions and incubated at 37 °C at for 24 h. The *Bacillus subtilis* suspensions with 10^4 CFU mL^{-1} concentration were chose as the control group. 100 μL of the mixture was taken out from the flask and diluted to ten times with sterilized natural seawater at each end of the incubation period for 0 h, 12 h. 100 μL of the decimal dilutions were spread on a petri dish that contained 2216E agar, and then incubated at 37 °C for 24 h. The number of bacteria colonies on each plate was counted. Three parallel experiments were set for each group of experiments.

To determine the anti-*Escherichia coli* activity of the HSI-EP-EU, we repeated the above operation and replace seawater with sterile 0.01 M phosphate buffer saline water and 2216E agar with nutrient agar.

$$\text{Antibacterial efficiency} = \frac{Nc - Ns}{Nc} \times 100\%$$

We marked the amount of microbial colonies on the plate without HSI-EP-EU as Nc, and the amount of microbial colonies on the plate with HSI-EP-EU as Ns.

To determine the antibacterial property of the cured P + HSI-EP-EU polymer and cured I + HSI-EP-EU polymer, the samples were placed in 24-well plates and seeded with 1000 μL of *Bacillus subtilis* sterilized natural seawater solution (10^8 CFU mL^{-1}), and incubated at 37 °C and 120 rpm for 24 h. The *Bacillus subtilis* on composite coating samples surface was stained *via* Calcein AM/PI kit and observed by fluorescent inverted microscope and SEM (the bacteria were fixed on the samples with glutaraldehyde solution (2.5 vol%) for 30 min (4 °C). Then the samples were sequentially wdehydrated with ethanol (15, 30, 50, 70, 90, 95 and 100 vol%) for 20 min, respectively).

We repeated the above experiment by replacing the *Bacillus subtilis* with *Escherichia coli* and replacing the sterilized natural seawater by the sterile 0.01 M phosphate buffer saline water to explore the anti-*Escherichia coli* activity of the P + HSI-EP-EU polymer and cured I + HSI-EP-EU polymer.

Results and discussion

Characterizations

The chemical structures of products were confirmed by FTIR and ^{1}H-NMR spectras. The FTIR spectrum (KBr) was collected with a Thermo Nicolet Nexus 6700 FTIR spectrometer instrument. ^{1}H-NMR spectra was obtained at room temperature on a 400 MHz AVANCE III NMR spectrometer in $CDCl_3$ with tetramethylsilane as internal reference. The viscosity of the EP/HSI-EP-EU was measured by a Physica MCR-301 rotary rheometer, and the angular frequency were set from 0.1 to 100 rad s. The DSC measurement was conducted on a NETZSCH 214 instrument under a nitrogen flow rate of 20 mL min^{-1} atmosphere and samples were heated from 298.15 to 523.15 °C (25 to 250 °C) at heating rates of 5, 10, 15, 20, 25 K min^{-1}, respectively. Thermal analysis of the P + HSI-EP-EU and I + HSI-EP-EU were performed by Netisch thermo gravimetric analysis (TGA). The thermal degradation behaviour was analyzed from 30 to 800 °C at a heating rate of 10 °C min under nitrogen flow rate of 200 mL min^{-1} atmosphere. Dynamic mechanical analysis (DMA) were performed on DMAQ800, and the rectangular samples (25 × 6.5 × 1.5 mm) were measured from room temperature to 200 °C at a heating rate of 3 °C min^{-1}, amplitude 2 μm, frequency 1 Hz. Tensile test was performed according to ASTM 638 using Universal Testing Machine (INSTRON 5869) with the crosshead speed of 2 mm min^{-1}. Five parallel samples were measured for each component. Characterization of bacteria staining experiments were conducted by biological laser confocal microscope (TCS SP5, LEICA, Germany). The concentration of bacteria is calibrated by SpectraMax 190 Microplate Reader. The surface morphology of bacteria was observed by the field emission SEM at high vacuum with 10.00 kV electric tension.

Characterization of HSI-EP-EU

The ^{1}H NMR spectra and FTIR spectra are shown in Fig. 1 and 2. As for Fig. 1a, the peaks at 5.04, 5.07 and 5.95 ppm (3a, b and 5) belonged to the C=C, after grafting epichlorohydrin, the peak at 5.5 ppm (4) completely disappears, and the formed peaks at 2.72 ppm (1a) and 2.87 ppm (1b) are attributed to the H atom introduced by epichlorohydrin (Fig. 1b). The FTIR spectra are shown in Fig. 2b and c also demonstrated the complete reaction of eugenol grafted epichlorohydrin. The specific result is that the –OH peak at 3518 cm^{-1} disappears in Fig. 2b, and appears the characteristic peak of epoxy group at 910 cm^{-1}. Then EP-EU is subjected to hydrosilylation reaction, and the ^{1}H NMR spectra show that the hydrogen atom on the double bond at 5.01 and 5.95 ppm (6a, 6b and 7) (Fig. 1b), and a new addition peaks of 0.50 and 0.90 ppm (1a, b, c and d and 2a, b and c) (Fig. 1c) belonged to the hydrogen atom on the ethyl group. FTIR spectra also have a corresponding verification of this process, and the peaks at 2109 and 720 cm^{-1} is belonged to the Si–H and Si–C in

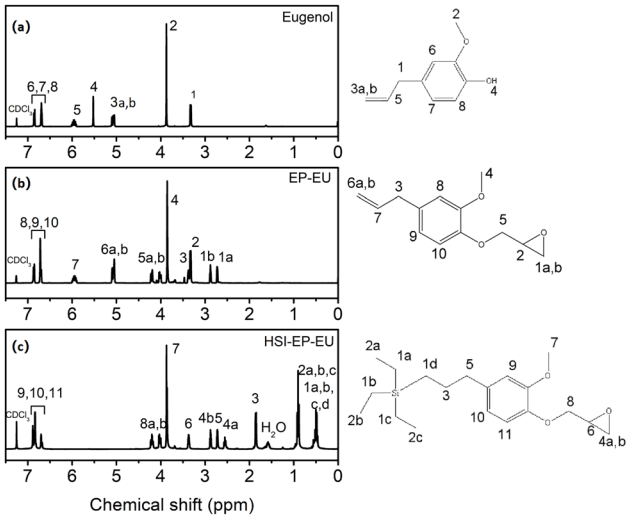

Fig. 1 ^{1}H NMR spectra of (a) eugenol, (b) EP-EU, and (c) HSI-EP-EU.

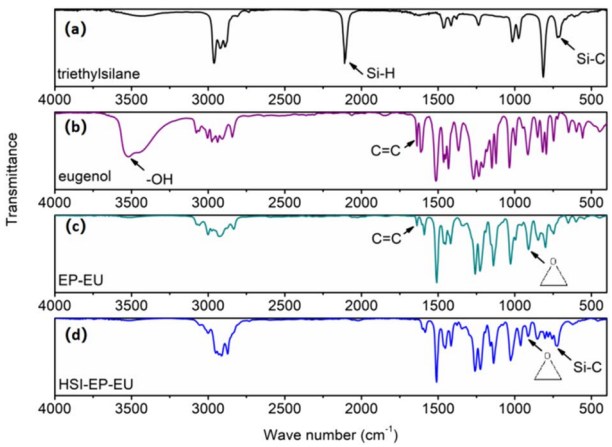

Fig. 2 FTIR spectra of (a) triethylsilane, (b) eugenol, (c) EP-EU, and (d) HSI-EP-EU.

Fig. 2a, and the characteristic peak of Si–C appeared in Fig. 2d, indicating that the reactive diluent HSI-EP-EU has been successfully synthesized.

The viscosity of the EP/HSI-EP-EU system

The viscosity of the epoxy system as a function of HSI-EP-EU addition is shown in Fig. 3. Pure HSI-EP-EU is a non-Newtonian fluid with the minimum viscosity of 181 mPa s (Fig. 3a) and the viscosity of neat EP is about 252 Pa s (Fig. 3b). It could be seen that the viscosity of the system shows a significant downward trend with the increase of the amount of HSI-EP-EU addition. The viscosity of EP/HSI-EP-EU system are 120 Pa s (5 wt% HSI-EP-EU), 84.4 Pa s (10 wt% HSI-EP-EU), 46.8 Pa s (15 wt% HSI-EP-EU) (Fig. 3b), respectively. Adding a small amount of HSI-EP-EU can significantly reduce the viscosity of the epoxy resin, which indicates that the excellent viscosity-reducing properties of HSI-EP-EU. When the mass fraction of diluent reaches 30%, the viscosity of system is reduced to 14.5 Pa s, which is 94% lower than that of the original system. Because the high viscosity epoxy prepolymer EP-44 contains a large amount of rigid benzene ring, restricting the movement of the long-chain molecular. The HSI-EP-EU molecular structure contains epoxy and structure of ether which bring the excellent compatibility with EP-44. The addition of HSI-EP-EU can destroy the original interaction force between the benzene rings, so that the long-chain molecules can be effectively unwound to weaken the rigidity of the system. In addition, the C–O, C–Si chemical bonds of the HSI-EP-EU could rotate freely. Therefore, as the content of HSI-EP-EU increases, the viscosity of the resin system decreases.

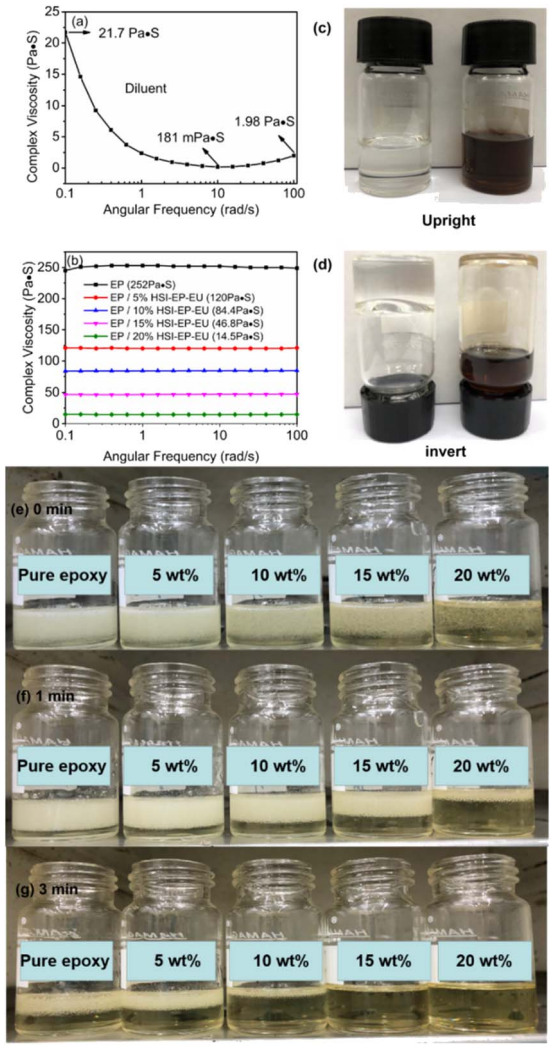

Fig. 3 The complex viscosity of (a) HSI-EP-EU, (b) EP/HSI-EP-EU system, (c) EP/HSI-EP-EU upright, (d), EP/HSI-EP-EU invert, (e) I + HSI-EP-EU processing performance at 0 min, (f) I + HSI-EP-EU processing performance for 1 min, (g) I + HSI-EP-EU processing performance for 3 min.

Processing performance of I + HSI-EP-EU system

The viscosity of the EP/HSI-EP-EU system has an important effect on the processing performance. The optical photographs are visually demonstrated the effect of HSI-EP-EU on the workability of EP-44. And we have put the EP-44 and HSI-EP-EU in two glass sample bottles. When the glass sample bottles are put upside down, HSI-EP-EU has excellent fluidity in the bottle and can be turned over instantly. On the contrary, EP-44 has only a tiny flow in the bottle (Fig. 3c and d). The polymer bubble removal process is monitored with the preparation of I+10 wt% HSI-EP-EU polymer. For the sample composition, we add the right amount of NMI and epoxy and 5 wt%, 10 wt%, 15 wt%, 20 wt% HSI-EP-EU. (Control group: only NMI and epoxy). The above components are uniformly mixed and placed in a vacuum oven at room temperature. As shown in Fig. 3(e), the bottle without HSI-EP-EU is wrapped with a lot of bubbles, the number of bubbles in the bottles is sequential decrement as the content of the HSI-EP-EU increased in the initial state. Using a vacuum pump to adjust the pressure of the vacuum oven to −0.1 MPa, the bubbles in all the bottles move up and the lower part of the mixture has gradually become clear. (Pressure: −0.1 MPa) (Fig. 3f). Maintaining the vacuum and prolonging the time, bubbles are firstly removed with 20 wt% HSI-EP-EU content, while the bubbles in other bottles are still observed (Fig. 3g). The epoxy resin has better processing performance with the addition of HSI-EP-EU.

The kinetic parameters of P + HSI-EP-EU and I + HSI-EP-EU

Isothermal and non-isothermal DSC methods are important methods for studying the curing kinetics of epoxy resins.[12] The kinetic parameters have high practical significance. In comparison, non-isothermal DSC methods can obtain the required kinetic data in a relatively short period of time and can determine the different heating rates.

It is well known that most acid anhydride curing agents are in a solid state at room temperature, and need to be dissolved in a liquid state at a certain temperature. In this work, HSI-EP-EU is chosen as a diluent in the epoxy system. The HHPA or NMI, 10 wt% HSI-EP-EU, DMP-30 and E-44 are mixed to form a homogenous solution for DSC test.

Fig. 4 has shown the non-isothermally cured DSC curves of the P + 10% HSI-EP-EU and I + 10% HSI-EP-EU system at

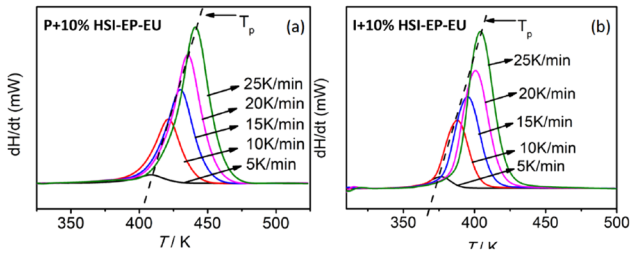

Fig. 4 DSC curves of (a) P + 10% HSI-EP-EU and (b) I + 10% HSI-EP-EU.

Table 1 Characteristic temperatures from DSC curves of P + HSI-EP-EU

β/K·min^{-1}	T_i/K	T_p/K	T_f/K
5	386.25	408.65	427.85
10	400.65	421.45	440.65
15	408.25	430.15	449.45
20	414.85	435.55	455.05
25	420.65	441.05	460.45

Table 2 Characteristic temperature from DSC curves of EP/NMI/HSI-EP-EU

β/K·min^{-1}	T_i/K	T_p/K	T_f/K
5	360.95	376.65	390.15
10	371.55	387.95	403.35
15	377.95	395.15	412.15
20	383.65	400.75	418.25
25	388.15	404.15	421.95

different heating rates. The corresponding thermodynamic parameters are listed in Table 1 and 2. By analyzing the exothermic peak change of the curing reaction at different heating rates, the characteristic temperature of curing reaction of each system, such as reaction initiation temperature (T_i), peak top temperature (T_p) and termination temperature (T_f) It could be seen that as the heating rate increases, the T_i, T_p, T_f gradually move toward the high temperature direction. Because the resin system stays at a fixed temperature for a short time at a rapid heating rate so that the degree of curing of resin is also reduced at this temperature. The accumulation of entire heating process causes the entire curve to move toward the high temperature.

Determination of kinetic parameters of P + HSI-EP-EU and I + HSI-EP-EU system

The structure and properties of the thermosetting resin obtained with different monomers and polymerization conditions are also different. Most thermosetting resins require practical use after adding a curing agent to make them into three-dimensionally crosslinked macromolecules. The structures and properties of macromolecules vary widely depending on the type, amount and curing conditions of curing agent. Therefore, it was of great practical significance to explore the curing behavior of thermosetting resins.[28,29] All thermosetting resin applications contain a curing reaction process, and the purpose of analyzing the curing reaction kinetics of P + 10% HSI-EP-EU and I + 10% HSI-EP-EU system are established the relationship between curing rate, curing degree with time and temperature to optimize the curing process.

In the curing process of epoxy resin, the determination of some curing kinetic parameters such as apparent activation energy E_α and reaction order n. E_α is an important parameter for determining a reaction how to proceed. According to the value of n, the complexity of the reaction and reaction mechanism can be easily determined.

In the thermal analysis process, the peak temperature of curing reaction under different heating rate conditions is determined by DSC analysis, and the values of apparent activation energy E_α and reaction order n are determined by the following two methods. Kissinger method is used the Kissinger equation to determine the value of E_α, and the value of n is obtained by the Crane formula. The other methods is Ozawa method similar to the Kissinger method.

The kinetic equations for epoxy systems all follow eqn (1). After differential processing, we could get eqn (2)

$$\frac{d\alpha}{dt} = K(T)(1-\alpha)^n \tag{1}$$

$$\ln\left(\frac{\beta}{T_p^2}\right) = \ln\left(\frac{AR}{E_\alpha}\right) - \left(\frac{E_\alpha}{RT_p}\right) \tag{2}$$

$$A = [\beta E_\alpha \exp(E_\alpha/RT_p)]/RT_p^2 \tag{3}$$

The value of $E_{\alpha1}$ (67.76 kJ mol^{-1}) and $E_{\alpha2}$ (67.86 kJ mol^{-1}) corresponding to P + 10% HSI-EP-EU and I + 10 wt% HSI-EP-EU are obtained by calculating the relationship between $\ln(\beta/T_p^2)$ and $1/T_p$ by linear fitting based on eqn (3) (Fig. 5a1 and a2). Then brought $E_{\alpha1}$ and $E_{\alpha2}$ into eqn (4), we could get two series of A values, listed in the Table 3 and Table 4.

When value of E_α/nR in the equation is much larger than the value of $2T_p$, the eqn (5) is simplified from the Crnae equation refer to the eqn (4). Then linear relationship between $\ln\beta$ and $1/T_p$ are calculated so that the slope and the number of reaction stages n are obtained. For the P + 10% HSI-EP-EU system, the slope 1 is −9000.00, $n_1 = 7$. In addition, for the I + 10% HSI-EP-EU system, the slope 2 is −8953.78, $n_2 = 0.912$.

$$\frac{d\ln\beta}{d(1/T_p)} = -(E_\alpha/nR + 2T_p) \tag{4}$$

$$\frac{d\ln\beta}{d(1/T_p)} = -\frac{E_\alpha}{nR} \tag{5}$$

The Ozawa eqn (6) is another curing kinetic model, which could be used to test and verify the activation energy value obtained by Kissinger equation.

$$\lg\beta = \lg\left[\frac{AE_\alpha}{Rf(\alpha)}\right] - 2.315 - 0.4567\frac{E_\alpha}{RT_p} \tag{6}$$

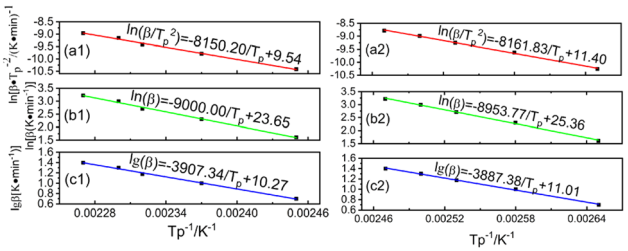

Fig. 5 (a1) The relation between (ln β/T_p^2) and $1/T_p$, (b1) the relation between ln β and $1/T_p$, (c1) and the relation between lg β and $1/T_p$ of P + 10% HSI-EP-EU. (a2) The relation between (ln β/T_p^2) and $1/T_p$, (b2) the relation between ln β and $1/T_p$, (c2) and the relation between lg β and $1/T_p$ of I + 10% HSI-EP-EU.

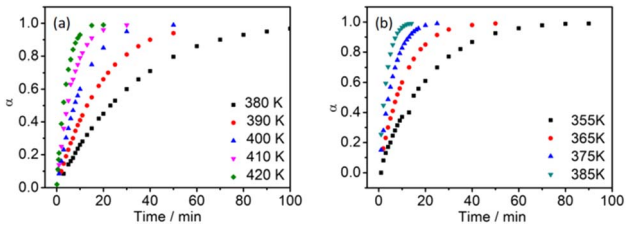

Fig. 6 The relation between α and t of (a) P + 10% HSI-EP-EU and (b) I + 10% HSI-EP-EU.

Since the A values at different heating rates are approximately the same, we have fitted the linear relationship between lg β and $1/T_p$, shown in Fig. 5. After calculation, we can get the value of $E_{\alpha 1}'$ and $E_{\alpha 2}'$ were 71.13 kJ mol^{-1} and 70.77 kJ mol^{-1}. The reaction activation energy obtained by these two methods are similar. The average reaction activation energy of P + 10% HSI-EP-EU and I + 10% HSI-EP-EU are 69.44 kJ mol^{-1} and 69.31 kJ mol^{-1}.

Dynamic equation of P + 10% HSI-EP-EU and I + 10% HSI-EP-EU system

$$K = A\exp(-E_\alpha/RT_p) \quad (7)$$

$$\frac{d(\alpha)}{d(t)} = A\exp(-E_\alpha/RT)(1-\alpha)^n \quad (8)$$

$$\alpha(t) = 1 - [1 + (n-1)A\exp(-E_\alpha/RT)t]^{\frac{1}{1-n}} \quad (9)$$

$$\alpha(t) = 1 - [1 - 9.79 \times 10^6 \exp(-8.56 \times 10^3/T)t]^{10.64} \quad (10)$$

$$\alpha(t) = 1 - [1 - 6.45 \times 10^7 \exp(-8.34 \times 10^3/T)t]^{11.36} \quad (11)$$

The eqn (9) is obtained by a series of mathematical derivations. The reaction activation energy and the reaction order number n are added into eqn (9). We have calculated the curing kinetic equations of the P + 10% HSI-EP-EU and I + 10% HSI-EP-EU systems. The relationship between α and t is determined by eqn (10) and (11) as shown in Fig. 6. The results are found that increasing reaction temperature (T) and prolonging reaction time (t) are equivalent to the curing process of P + 10% HSI-EP-EU and I + 10% HSI-EP-EU. In other words, the conversion rate (α) has time and temperature dependence.

Curing temperature of P + 10% HSI-EP-EU and I + 10% HSI-EP-EU

The curing temperatures are obtained at the heating rate of 0 K min^{-1} by T–β extrapolation as the reliable curing temperature of the system. The value of heating rate are taken as the horizontal coordinate, and the values of T_i, T_p and T_f are taken as the vertical coordinates to obtain the linear relationship, and shown in Fig. 7. As for P + 10% HSI-EP-EU system Fig. 7a1, b1 and c1, we find the peak starting temperature is 381.23 K (gel

Table 3 The kinetics parameters of P + HSI-EP-EU curing reaction

β/K min^{-1}	ln(β/T_p^2)/(K min^{-1})	ln β/(K min^{-1})	lg β/(K min^{-1})	T_p^{-1}/K^{-1} (10^{-5})	A min^{-1} (10^8)
5	−10.416	1.609	0.699	245	0.677
10	−9.785	2.303	1.000	237	1.147
15	−9.420	2.708	1.176	232	1.118
20	−9.157	2.996	1.301	230	1.150
25	−8.959	3.219	1.398	227	1.110
Average					1.040

Table 4 The kinetics parameters of I + HSI-EP-EU curing reaction

β/K min^{-1}	ln(β/T_p^2)/(K min^{-1})	ln β/(K min^{-1})	lg β/(K min^{-1})	T_p^{-1}/K^{-1} (10^{-5})	A min^{-1} (10^8)
5	−10.254	1.609	0.699	265	7.41
10	−9.619	2.303	1	258	7.43
15	−9.250	2.708	1.176	253	7.32
20	−8.991	2.996	1.301	250	7.11
25	−8.785	3.219	1.398	247	7.37
Average					7.33

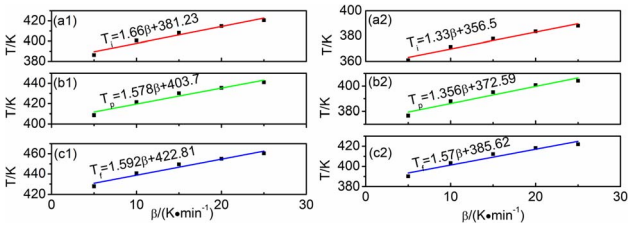

Fig. 7 The extrapolation plots of β–T: P + 10% HSI-EP-EU (a1) T_i, (b1) T_p, (c1) T_f; I + 10% HSI-EP-EU (a2) T_i, (b2) T_p, (c2) T_f.

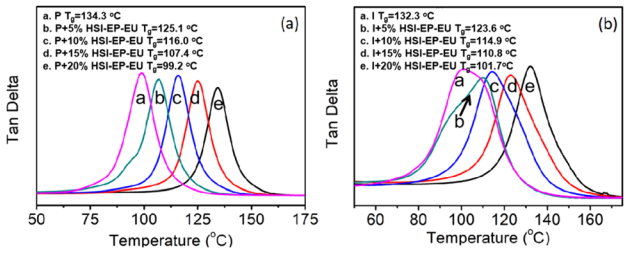

Fig. 9 Tan δ *versus* temperature plots of (a) P + HSI-EP-EU and (b) I + HSI-EP-EU.

temperature 108.08 °C), the peak temperature is 403.70 K (curing temperature 130.55 °C), and the peak end temperature is 422.81 K (post-cure temperature 149.66 °C). The best curing conditions for P + 10% HSI-EP-EU were 110 °C for 1 h, at 130 °C for 2 h and at 150 °C for 3 h. For the same method in I + 10% HSI-EP-EU system Fig. 7a2, b2 and c2, the best curing conditions are as 80 °C for 1 h, at 100 °C for 2 h and at 110 °C for 3 h.

Thermal stability

The thermal stability of cured epoxy are analyzed by TGA analysis. The information obtained by the controlled degradation of the polymer could be used to evaluate whether a given material will be useful for a high temperature potential application. As shown in Fig. 8, no significant difference between the oxidation of resin side chain and the carbonization of main chain appears with the increase of HSI-EP-EU content. Comparison of two sets of curing agent systems, there is no difference in thermal decomposition behavior of two systems before 150 °C. With the increasing temperature, the difference in thermal decomposition properties of the materials has gradually emerged due to the different curing agents. And the system cured by the NMI curing agent had better thermal stability. When both systems weight loss reached 20%, the HHPA cured material at a decomposition temperature (T_{d80}) of 395 °C and an NMI curing system T_{d80} is 410 °C. And when the weight loss reached 85%, the corresponding temperatures (T_{d85}) are 450 and 465 °C, respectively.

Dynamic mechanical properties

DMA is employed to study the thermal properties of P + HSI-EP-EU and I + HSI-EP-EU resin systems. Fig. 9 has presented the tan delta curves at a function of temperature for epoxy resin without and with different contented of HSI-EP-EU. The glass transition temperature (T_g) of polymer is identified as the peak of tan delta curve. It is obviously that all the HSI-EP-EU containing the cured product exhibit the decreased in T_g as observed from the shifts of tan delta peaks to the low temperature region. As for the P + HSI-EP-EU, pure epoxy resin has a T_g of 134.3 °C, the T_g of the cured product after adding HSI-EP-EU has decreased to 125.1 °C (5 wt%), 116.0 °C (10 wt%), 107.4 °C (15 wt%), 99.2 °C (20 wt%), respectively. Similar results have been observed from I + HSI-EP-EU system, the T_g of cured product behaved as 132.3 °C (0 wt%), 123.6 °C (5 wt%), 114.9 °C (10 wt%), 110.8 °C (15 wt%), 101.7 °C (20 wt%). The reduced T_g is associated with the declined of the polymer chains mobility caused by the C–O and O–Si chemical bonds carried in the HSI-EP-EU molecule with great rotational flexibility.

The mechanical properties

The tensile properties of the P + HSI-EP-EU and I + HSI-EP-EU system are determined by stress–strain measurements. The typical strain–stress plots for the pure epoxy and epoxy containing 5, 10, 15 and 20 wt% HSI-EP-EU are shown in Fig. 10. And the tensile properties, including tensile strength, Young's modulus and strain-to-break are given in Table 5 and 6.

It could be easily seen that the addition of HSI-EP-EU has different effects on the mechanical properties of the two curing agents system. For the P + HSI-EP-EU system, the addition of the HSI-EP-EU has led to a nearly complete decline in the mechanical properties of the cured product (including tensile strength, tensile modulus, elongation at break), and only a slight increase in elongation at break. Because the anhydride-cured epoxy resin is strong enough and difficult to be increased the strength and modulus by adding a flexible diluent. As shown in Fig. 10a and b, the longation at break of the material can be improved with addition of flexible HSI-EP-EU (5 wt%,

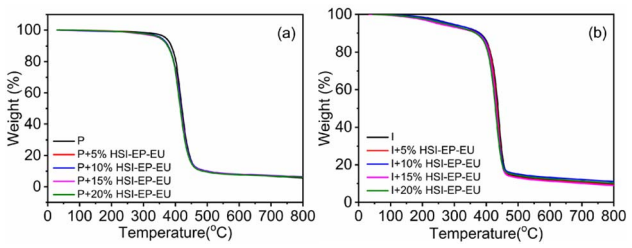

Fig. 8 TGA curves of (a) P + HSI-EP-EU and (b) I + HSI-EP-EU.

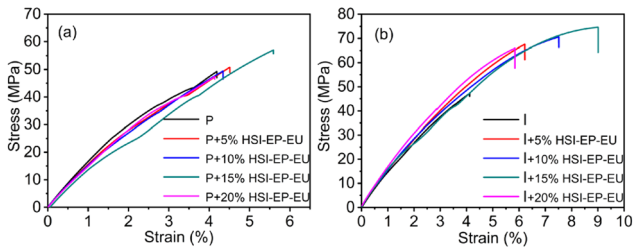

Fig. 10 Stress–strain curves of (a) P + HSI-EP-EU and (b) I + HSI-EP-EU.

Table 5 Tensile properties of P + HSI-EP-EU

Sample	Tensile strength/MPa	Strain at break/%	Tensile modulus/MPa
P	57.0 ± 3.2	4.2 ± 0.2	1933 ± 32
P + 5% HSI-EP-EU	49.3 ± 3.4	4.5 ± 0.4	1916 ± 47
P + 10% HSI-EP-EU	49.4 ± 2.7	4.3 ± 0.1	1756 ± 43
P + 15% HSI-EP-EU	55.7 ± 1.2	5.6 ± 0.3	1745 ± 56
P + 20% HSI-EP-EU	47.4 ± 2.5	4.1 ± 0.2	1651 ± 38

Table 6 Tensile properties of I + HSI-EP-EU

Sample	Tensile strength/MPa	Strain at break/%	Tensile modulus/MPa
I	47.2 ± 1.6	4.1 ± 0.8	1637 ± 45
I + 5% HSI-EP-EU	67.6 ± 0.4	6.2 ± 0.1	2071 ± 58
I + 10% HSI-EP-EU	70.6 ± 1.8	7.5 ± 0.7	1852 ± 33
I + 15% HSI-EP-EU	74.6 ± 2.9	9.0 ± 0.3	1954 ± 67
I + 20% HSI-EP-EU	66.0 ± 3.4	5.8 ± 0.9	2039 ± 40

10 wt%, 15 wt%). When we add a flexible diluent HSI-EP-EU (20 wt%), it results in a decrease in elongation at break, which may have affected the cross-link density of the material. According to Scheme 2, HSI-EP-EU has an epoxy group, and each epoxy group after ring opening will be connected with two acid anhydride molecules, adding HSI-EP-EU, it will consume more acid anhydride curing agent. Moreover, the HSI-EP-EU entering the linear molecule of the epoxy resin will extend the entire molecular chain, thereby weakening the reinforcing effect of the rigid acid anhydride molecule in the entire system. It results in a decrease in the mechanical properties of system.

When the curing agent is selected as NMI, the cured product with no diluent HSI-EP-EU possess strength of 47.2 MPa, the elongation at break is 4.1%, and the tensile modulus is 1637 MPa. The addition of reactive diluent HSI-EP-EU could improve the mechanical properties of the material. The enhancement of both modulus, tensile strength and elongation at break are prominent with HSI-EP-EU loading in epoxy matrices without scarifying its strain to failure. With addition of 5 wt% HSI-EP-EU into epoxy matrix, tensile modulus are enhanced by 43.2% (from 47.2 to 67.6 MPa) and 26.5% (from 1637 to 2071 MPa), respectively.

Compared with I group, the tensile strength of I + 15% HSI-EP-EU is improved 58.1% (from 47.2 to 74.6 MPa) with addition of 15 wt% HSI-EP-EU. And elongation at break of I + 15% HSI-EP-EU is more than doubled enhanced compared with neat epoxy resin.

There are 1-position secondary amine nitrogen atom and 3-position tertiary amine nitrogen atom in the molecular structure of imidazole curing agent. When curing epoxy resin, it is generally believed that the 3-position nitrogen atom on the imidazole ring firstly opens the epoxy group in the epoxy resin. For 1-methylimidazole, when there is a methyl substituent on the 1-position nitrogen atom, the 1-position nitrogen atom does not react with the epoxy resin, and only the 3-position nitrogen atom opens the epoxy group in the epoxy resin. Finally, the oxygen anions generated by the ring-opening of epoxy groups continue to catalyze the ring-opening polymerization of epoxy resins. According to Scheme 3, HSI-EP-EU has an epoxy group, and when the imidazole molecule initiates anionic polymerization of the epoxy group, the epoxy group of HSI-EP-EU will be introduced into the cross-linked network. An appropriate amount of HSI-EP-EU will increase the cross-linking density of the whole system, the number of chemical bonds will increase, and the entanglement between molecular chains will be more serious, which will improve the mechanical properties of the cured product. When the amount of HSI-EP-EU is excessive, the size of the cross-linking lattice will continue to expand, which may lead to the decrease of the cross-linking density. Even if there is free HSI-EP-EU in the system, these small molecules will produce plasticization, thereby deteriorating the overall mechanical properties of the material. This means that the effect of excess HSI-EP-EU in the system is somewhat similar to that of non-reactive diluents. Addition of the non-reactive (toluene) diluents[27] in epoxy resin formed large number of plastic deformation zones to the incorporation flexible network, which further reduced the mechanical properties of the epoxy resin system. In summary, HSI-EP-EU is proved to be an effective diluent system in EP/NMI system and can be used as suitable diluent for high-performance application.

Antibacterial property test of HSI-EP-EU, cured P + 15% HSI-EP-EU polymer and cured I + 15% HSI-EP-EU polymer

The agar well diffusion method, standard plate count method is conducted for exploring the antibacterial activity of HSI-EP-EU. As shown in Fig. 11a and f, under the action of HSI-EP-EU, the culture medium containing *Escherichia coli* and *Bacillus subtilis* both emerged a zone of inhibition. This indicates that HSI-EP-EU has the inhibitory effect on both Gram-negative bacteria and Gram-positive bacteria. Antibacterial efficiency of HSI-EP-EU is assessed by counting the colonies of bacteria

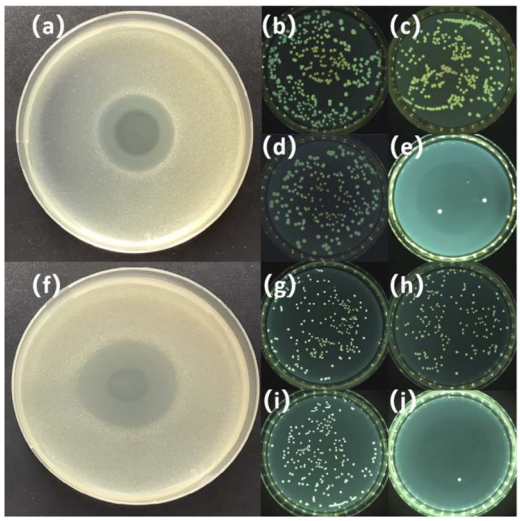

Fig. 11 Antibacterial property test of HSI-EP-EU, (a) zone of inhibition for *Escherichia coli*, (b) colonies of *Escherichia coli* without HSI-EP-EU at 0 h, (c) colonies of *Escherichia coli* without HSI-EP-EU at 12 h, (d) colonies of *Escherichia coli* with HSI-EP-EU at 0 h, (e) colonies of *Escherichia coli* with HSI-EP-EU at 12 h, (f) zone of inhibition for *Bacillus subtilis*, (g) colonies of *Bacillus subtilis* without HSI-EP-EU at 0 h, (h) colonies of *Bacillus subtilis* without HSI-EP-EU at 12 h, (i) colonies of *Bacillus subtilis* with HSI-EP-EU at 0 h, (j) colonies of *Bacillus subtilis* with HSI-EP-EU at 12 h.

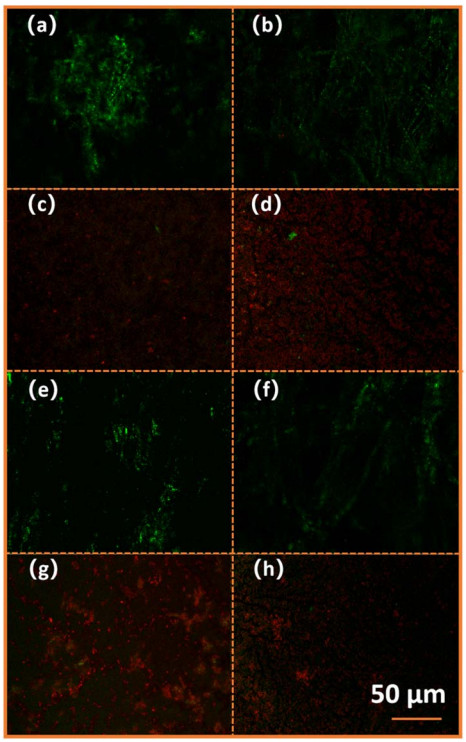

Fig. 12 Antibacterial property test of (a) cured P + 15% HSI-EP-EU polymer against *Escherichia coli* at 0 h, (b) cured I + 15% HSI-EP-EU polymer against *Escherichia coli* at 0 h, (c) cured P + 15% HSI-EP-EU polymer against *Escherichia coli* at 24 h, (d) cured I + 15% HSI-EP-EU polymer against *Escherichia coli* at 24 h, (e) cured P + 15% HSI-EP-EU polymer against *Bacillus subtilis* at 0 h, (f) cured I + 15% HSI-EP-EU polymer against *Bacillus subtilis* at 0 h, (g) cured P + 15% HSI-EP-EU polymer against *Bacillus subtilis* at 24 h, (h) cured I + 15% HSI-EP-EU polymer against *Bacillus subtilis* at 24 h by live/dead imaging.

in solution before and after HSI-EP-EU treatment. HSI-EP-EU is added to the experimental group (*Escherichia coli* initial concentration of 10^4 CFU mL^{-1}) with a concentration of 2.5 μL mL^{-1}, the bacterial colonies appears on the petri dishes with the number of 264 (0 h) (Fig. 11d). After 12 h, only two bacterial colonies appears on the petri dishes (Fig. 11e). It is shown that *Escherichia coli* is killed within 12 hours of exposure to HSI-EP-EU. The antibacterial efficiency of HSI-EP-EU against *Escherichia coli* is ≥ 99.0%. The control medium (Fig. 11b and c) has no toxic effect on *Escherichia coli*, which is consistent with *Bacillus subtilis* (Fig. 11g and i). The antibacterial efficiency of HSI-EP-EU against *Bacillus subtilis* is also ≥99.0%.

We have already known that HSI-EP-EU has the excellent bactericidal properties against both Gram-negative and Gram-positive bacteria. Therefore, HSI-EP-EU is combined with the traditional commercial epoxy E44 to produce an advanced composite coating with bactericidal properties. Scanning electron microscopy and live/dead cell staining techniques is used to investigate the poisoning effect for *Escherichia coli* and *Bacillus subtilis* on the surface of the cured P + 15% HSI-EP-EU polymer and cured I + 15% HSI-EP-EU polymer as the typical research objects.

For cured P + 15% HSI-EP-EU polymer (Fig. 12a and c) and cured I + 15% HSI-EP-EU polymer (Fig. 12b and d) against *Escherichia coli*, there is a lot of green fluorescence under the excitation of specific wavelength fluorescence with a few red fluorescent spots observed (Fig. 12a and b) at the 0 h. The red fluorescence is caused by *Escherichia coli*, which is apoptotic in the normal life cycle. After 24 h, the fluorescence microscope observation results are opposite to it from the initial phase. The vast majority of field of view is red, and only a few particles shows green fluorescence (Fig. 12c and d). For cured P + 15% HSI-EP-EU polymer (Fig. 12e and g) and cured I + 15% HSI-EP-EU polymer (Fig. 12f and h) against *Bacillus subtilis*, we obtained experimental results are similar to *Escherichia coli*. The cured P + 15% HSI-EP-EU polymer and cured I + 15% HSI-EP-EU polymer have excellent killing effect on *Escherichia coli* and *Bacillus subtilis*. By adding active diluent HSI-EP-EU, we can give it advanced antibacterial function while improving the construction performance of traditional commercial E44.

SEM images of bacterial morphology are provided in Fig. 13. The original *Bacillus subtilis* (Fig. 13a) and *Escherichia coli* (Fig. 13d) display intact membranes. When the *Bacillus subtilis* and *Escherichia coli* are attached on the surface of P + 15% HSI-EP-EU and I + 15% HSI-EP-EU polymer, respectively, cell membranes show various degrees of deformation such as wrinkles and even cracks (Fig. 13b, c, e and f), along with the cytoplasm leakage of bacteria (Fig. 13b and c). Negative charges of bacterial surface can be attracted by positive charges from I +

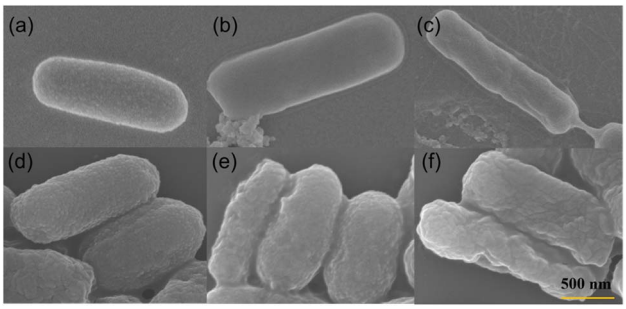

Fig. 13 SEM images of (a) original *Bacillus subtilis*, (b) cured P + 15% HSI-EP-EU polymer against *Bacillus subtilis* at 24 h, (c) cured I + 15% HSI-EP-EU polymer against *Bacillus subtilis* at 24 h, (d) original *Escherichia coli*, (e) cured P + 15% HSI-EP-EU polymer against *Escherichia coli* at 24 h, (f) cured I + 15% HSI-EP-EU polymer against *Escherichia coli* at 24 h.

15% HSI-EP-EU polymer materials, restricting the activities of bacteria and lead to the death of bacteria.[30,31]

Conclusions

Hydrosilylation epoxidized eugenol (HSI-EP-EU) is successfully synthesized and used as reactive diluent for epoxy/anhydride, and epoxy/imidazole curing system. Based on curing kinetic studies, the value of pre-exponential factor A, apparent activation energy E_α, reaction stages n are calculated. According to the results of the extrapolation of T–β method, the curing temperatures of two curing systems are determined. For the epoxy/anhydride curing system, the best curing conditions is 110 °C for 1 h, at 130 °C for 2 h and at 150 °C for 3 h. The addition of HSI-EP-EU could reduce the mechanical properties of the anhydride cured product. In regard to the epoxy/imidazole curing system, best curing conditions is 80 °C for 1 h, at 100 °C for 2 h and at 110 °C for 3 h. The addition of a HSI-EP-EU could improve the mechanical properties of imidazole cured product. HSI-EP-EU has the excellent bactericidal properties against both Gram-negative and Gram-positive bacteria. We can give it advanced antibacterial function of traditional commercial E44 by adding active diluent HSI-EP-EU.

Author contributions

Jingyu Li: conceptualization, investigation, project administration, formal analysis, software, methodology, data curation, writing-original draft. Haichao Zhao: conceptualization, supervision, project administration, formal analysis, data curation, writing-review & editing, funding acquisition. Guoxin Sui: conceptualization, supervision, project administration, formal analysis, data curation, writing-review & editing, funding acquisition.

Conflicts of interest

The authors declare that they have no known competing financial interests or personal relationships that could have appeared to influence the work reported in this paper.

Acknowledgements

The authors gratefully acknowledged financial support provided by "One Hundred Talented People" of The Chinese Academy of Sciences-China (No. Y60707WR04), Zhejiang Key Research and Development Program (2022C01213) and Graduate Innovation Research Fund of Institute of Metal Research, Chinese Academy of Sciences (1193002090).

References

1 H. Wang, C. Li, Z. Hou, B. Li and H. Cai, *RSC Adv.*, 2022, **12**, 7046–7054.
2 A. Toldy, B. Szolnoki and G. Marosi, *Polym. Degrad. Stab.*, 2011, **96**, 371–376.
3 A. Saccani, S. Manzi, I. Lancellotti and L. Lipparini, *Constr. Build. Mater.*, 2019, **204**, 296–302.
4 P. Antil, S. Singh, S. Kumar, A. Manna and C. Pruncu, *Mater. Res. Express*, 2019, **6**, 106520.
5 T. H. Huang, J. J. Yang, H. Li and C. T. Kao, *Biomaterials*, 2002, **23**, 77–83.
6 D. Yamazaki, M. Iwanami and M. Isa, *J. Adv. Concr. Technol.*, 2020, **18**, 463–472.
7 F. Yu, H. Feng, L. Xiao and Y. Liu, *Prog. Org. Coat.*, 2021, **155**, 106221.
8 A. Javaid, O. Khalid, A. Shakeel and S. Noreen, *J. Energy Storage*, 2021, **33**, 102168.
9 B. Chen, J. Li, X. Li, T. Liu, Z. Dai, H. Zhao and L. Wang, *Polym. Compos.*, 2018, **39**, E2407–E2414.
10 N. Gupta and W. Ricci, *J. Mater. Process. Technol.*, 2008, **198**, 1–3.
11 B. Chen, F. Wang, J. Y. Li, J. L. Zhang, Y. Zhang and H. C. Zhao, *Chin. J. Polym. Sci.*, 2019, **37**, 500–508.
12 C. Li, M. H. Liu, Z. Y. Liu, M. L. Qing and G. Wang, *J. Therm. Anal. Calorim.*, 2014, **116**, 411–416.
13 A. F. E Pineda, F. G. Garcia, A. Z. Simões and E. L. D. Silva, *Int. J. Adhes. Adhes.*, 2016, **68**, 205–211.
14 A. Asekomeh, O. Gershon and S. I. Azubuike, *Energies*, 2021, **14**, 1–23.
15 J. H. Clark, *Green Chem.*, 2006, **8**, 17–21.
16 A. D. Tran, T. Koch, P. Knaack and R. Liska, *Composites, Part A*, 2020, **132**, 105855.
17 S. K. Sahoo, V. Khandelwal and G. Manik, *Polym. Adv. Technol.*, 2018, **29**, 565–574.
18 F. Hu, J. Scala, J. M. Sadler and G. R. Palmese, *Macromolecules*, 2014, **47**, 3332–3342.
19 J. Ding, W. Peng, T. Luo and H. Yu, *RSC Adv.*, 2017, **7**, 6981–6987.
20 W. Huang, X. Liu, J. Zhu and Q. Cao, *Chem. Bull.*, 2011, **74**, 92–96.
21 A. U. Yap, K. C. Shah, E. T. Loh, S. S. Sim and C. C. Tan, *Operat. Dent.*, 2001, **26**, 556–561.
22 J. Zheng, Y. Cai, X. Zhang, J. Wan and H. Fan, *ACS Appl. Polym. Mater.*, 2022, **4**, 929–938.
23 C. Li, H. Fan, T. Aziz, C. Bittencourt, L. Wu, D. Y. Wang and P. Dubois, *ACS Sustainable Chem. Eng.*, 2018, **6**, 8856–8867.

24 J. Qin, H. Liu, P. Zhang, M. Wolcott and J. Zhang, *Polym. Int.*, 2014, **63**, 760–765.
25 C. François, S. Pourchet, G. Boni, S. Rautiainen, J. Samec, L. Fournier, C. Robert, C. M. Thomas, S. Fontaine and Y. Gaillard, *C. R. Chim.*, 2017, **20**, 1006–1016.
26 X. Fu, Y. Gao, W. Yan, Z. Zhang, S. Sarker, Y. Yin, Q. Liu, J. Feng and J. Chen, *RSC Adv.*, 2022, **12**, 3180–3190.
27 A. Sinha, N. I. Khan, S. Das, J. Zhang and S. Halder, *High Perform. Polym.*, 2018, **30**, 1–10.
28 D. Roşu, C. Caşcaval, F. Mustaţă and C. Ciobanu, *Thermochim. Acta*, 2002, **383**, 119–127.
29 R. L. Pagano, V. M. A. Calado, F. W. Tavares and E. C. Biscaia, *J. Therm. Anal. Calorim.*, 2011, **103**, 495–499.
30 P. K. Samantrary, G. Madras and S. Bose, *Adv. Sustainable Syst.*, 2019, 1900017.
31 S. S. Nair, V. Anand, K. D. Silva, S. Wiles and S. Swift, *J. Appl. Microbiol.*, 2022, 1–16.